Vibrational State-to-State Modeling of a Recombining Nitrogen/Argon Plasma

Pierre Mariotto, A C Tibère-Inglesse, S Mcguire, Marie-Yvonne Perrin, Christophe O Laux, Rowan Gollan, Peter Jacobs

AIAA SciTech Forum
7-11 January 2019, San Diego, California
AIAA Scitech 2019 Forum

10.2514/6.2019-0796

Vibrational State-to-State Modeling of a Recombining Nitrogen/Argon Plasma

P. Mariotto[1], A. Tibère-Inglesse[2], S. McGuire[3], M.Y. Perrin[4] and C.O. Laux[5]
Laboratoire EM2C, CNRS UPR288, CentraleSupélec, Université Paris-Saclay, 10 rue Joliot-Curie, 91190, Gif-sur-Yvette, France

P. Jacobs[6], R. Gollan[7]
School of Mechanical and Mining Engineering, University of Queensland, 4076 St Lucia, Australia

A vibrational state-to-state kinetic model is developed and compared with recent measurements performed in a nitrogen/argon recombining plasma at atmospheric pressure. It is shown that the flow experiences high vibrational non-equilibrium, which slows down the recombination process of nitrogen atoms. The present state-to-state model overpredicts the experimental atomic nitrogen densities.

I. Introduction

During atmospheric reentry, spacecraft experience high convective and radiative heat fluxes. Reliable kinetics models are required to predict both quantities, because they influence the energy balance and the population of radiating levels.

Computational fluid dynamics (CFD) codes [1]–[4] generally use *chemical models* based on empirical fits of shock tube data [5]–[7]. These models describe non-equilibrium effect only crudely, because internal energy levels are assumed to follow Boltzmann distributions (typically for a 2-temperature model, electronic-vibrational levels and rotational-translational levels follows Boltzmann distributions at $T_{vib} = T_{el}$ and $T_{tr} = T_{rot}$ respectively). Recent advances in computational chemistry enable to reconsider these models from *ab initio* methods [8]–[10] and to develop *state-to-state models (StS).* The StS models can account for non-equilibrium chemistry, where internal energy levels can depart from Boltzmann distributions. Vibrational levels can be treated as pseudo-species, with populations obtained by solving the master equation.

Recently, experiments were performed to provide well-defined test cases to validate CFD codes and reactions mechanisms for recombining flows. In particular, the recombination of an N_2/Ar plasma was studied experimentally at Stanford [11]–[13], and the same facility was used recently in CentraleSupélec to confirm and extend the Stanford results [14], [15].

Chemical reactions mechanisms from Park, Gupta and Dunn have been compared against experimental data in [11]–[13]. It was shown that the limiting recombination reaction is $N_2 + M \rightleftharpoons N + N + M$ with $M = N, N_2$, and Ar. The authors concluded that Park's model was closest to their experimental results but that there were still discrepancies.

In the present paper, we repeat the same analysis as in [11], [12] with the new set of measurements obtained at CentraleSupélec and reported in [15]. Then we extend the study by comparing chemical and StS models on this updated test case.

II. Experimental setup and measurements

A 50 kW TAFA model 66 radio-frequency inductively-coupled plasma torch, powered by a LEPEL model T-50-3 power supply operating at a frequency of 4 MHz, was used to generate air, nitrogen/argon, and air/argon plasmas at atmospheric pressure. The plasmas produced in the torch exit through a 1 cm diameter copper nozzle at velocities up to 1 km/s, and then flow through a water-cooled, 1 cm diameter brass test-section mounted on the

[1] Ph.D. Candidate, EM2C, CentraleSupélec, Université Paris-Saclay and Center for Hypersonics, School of Mechanical and Mining Engineering
[2] Ph.D. Candidate, EM2C, CentraleSupélec, Université Paris-Saclay and ArianeGroup (Les Mureaux, France)
[3] Assistant Professor, EM2C, CentraleSupélec, Université Paris-Saclay, AIAA Member
[4] Senior Researcher at CNRS
[5] Professor, EM2C, CentraleSupélec, Université Paris-Saclay, AIAA Associate Fellow
[6] Lecturer, Center for Hypersonics
[7] Lecturer, Center for Hypersonics

exit nozzle of the torch as shown in Figure 1. The test-section consists of two brass tubes separated by a 3 mm thick annular water cooling passage. Within the test-section, the plasmas are forced to recombine in a well-controlled environment over a predetermined residence time

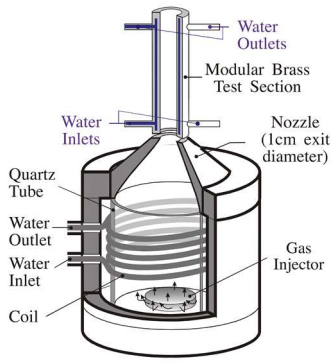

Figure 1 : Schematic cross-section of torch head with test-section

The experiments are presented in detail in [16]. Here, we focus on the case of the nitrogen/argon plasma. In the experiments, the flowrate of nitrogen N_2 is 90 slpm, and the flowrate of argon Ar is 50 slpm. Temperature along the centerline was measured by optical emission spectroscopy and Raman scattering. Atomic nitrogen N densities along the centerline were deduced from the measurements of $N_2(B, v = 13)$ density, assuming that the predissociation reaction $N_2(B, v = 13) \rightleftharpoons N(\,^4S) + N(\,^4S)$ is equilibrated [17]. N densities at various locations along the tube axis ($x = 0\ cm$ corresponding to the entrance of the tube) are reported in the second column of Table 1.

Axial location $x\ [cm]$	N densities $[m^{-3}]$	$t\ [\mu s]$ constant $U(r)$	$t\ [\mu s]$ CFD $U(r)$	$t\ [\mu s]$ Parabolic $U(r)$
0	$4.46 \cdot 10^{23}$	0	0	0
10	$1.83 \cdot 10^{23}$	247	169	112
15	$1.28 \cdot 10^{23}$	405	276	184

Table 1 : Atomic nitrogen densities and times to reach the observation locations.

III. Results

A. Kinetics models

Two kinetic models are compared in this paper: the first one, called *chemical model*, considers that internal levels are populated according to Boltzmann distributions. The second one, called the *state to state model (StS model)*, is vibrationally specific and tracks each vibrational level separately.

1. Chemical model

The chemical model (CM) includes the following reactions whose coefficients are listed in Table 2:

$$\begin{cases} N_2 + N \rightleftharpoons N + N + N \\ N_2 + N_2 \rightleftharpoons N + N + N_2 \\ N_2 + Ar \rightleftharpoons N + N + Ar \end{cases}$$

The rate of dissociation of N_2 by N impact is taken from an Arrhenius fit of Esposito's data [10]. The data of Esposito were computed by the quasi-classical trajectory method (QCT). A global rate k_d can be obtained by summing over the vibrational levels populations:

$$k_d^{N2-N}(T) = \sum_v \frac{n_v}{n_{tot}} \cdot k_d(v) \tag{1.1}$$

where

$$\frac{n_v}{n_{tot}} = \frac{\exp\left(-\frac{G(v)}{k_b T}\right)}{\sum_v \exp\left(-\frac{G(v)}{k_b T}\right)} \tag{1.2}$$

n_v and n_{tot} are the densities of the vibrational level $N_2(X, v)$ and the total density respectively. $G(v)$ is the energy of $N_2(X, v, J = 0)$. $k_d(v)$ is the dissociation rate of $N_2(X, v)$. Excellent agreement is obtained with Park's rate [5]. The following model (StS model) will be based on vibrationally specific dissociation rates $k_d(v)$ to compute recombination/dissociation in a state-specific way. Dissociation rates of N_2 by N_2 and Ar impact have been derived by multiplying k_d^{N2-N} by the scaling factors $\eta_{N_2-N_2} = k_d^{N_2-N_2}/k_d^{N_2-N} = 1$ [9] and $\eta_{N_2-Ar} = k_d^{N_2-Ar}/k_d^{N_2-N} = 0.1$ [18] respectively. However, unlike in Ref. [18], we set $\eta_{N_2-N_2} = 1$ because recent QCT calculations [9] showed that N_2 dissociates N_2 with the same efficiency as N. The authors of Ref. [9] explain that the previous assumption was based on experimental results that may have been biased by non-equilibrium in the high-lying vibrational states.
The backward rates are computed using the equilibrium constants, which are computed from the Gordon and McBride [19] curve fits of enthalpy and entropy.

Reaction	M third body	$A\ [cm^3/s]$	n	$E\ [K]$	$\eta = \frac{k^{N_2-M}}{k^{N_2-N}}$
$N_2 + M \rightleftharpoons N + N + M$	N	$1.7004 \cdot 10^{-7}$	-0.095333	113700	1.0
	N_2	$1.7004 \cdot 10^{-7}$	-0.095333	113700	1.0
	Ar	$0.1700 \cdot 10^{-7}$	-0.095333	113700	0.1

Table 2 : Forward rate coefficient in Arrhenius Form $k_d(T) = A \cdot T^n \cdot e^{-\frac{E}{T}}\ [cm^3/s]$. Coefficients for $M = N$ are from [10] **and other A are obtained by multiplying the A coefficient for N by η** [9], [18]**.**

2. State-to-state model

The state-to-state model tracks each vibrational level as a pseudo species. The model includes the following reactions:

- dissociation from each vibrational level by N, N_2 and Ar impact:
  $N_2(X\ ^1\Sigma^+, v) + M \rightleftharpoons N + N + M\ \forall\ v \in [\![0, v_{max}]\!],\ M \in [N, N_2, Ar]$. Forward rates are taken from Esposito's QCT results [10] and colliders efficiencies (which are assumed independent of the vibrational level v) are taken from Table 2.
- vibration-translation (VT) exchange:
  $N_2(X\ ^1\Sigma^+, v) + N \rightleftharpoons N_2(X\ ^1\Sigma^+, v') + N\ \forall\ (v, v') \in [\![0, v_{max}]\!]^2\ v \neq v'$. Forward rates are taken from Esposito's QCT results [10].
- vibration-translation (VT) exchange:
  $N_2(X\ ^1\Sigma^+, v) + M \rightleftharpoons N_2(X\ ^1\Sigma^+, v-1) + M, M \in [N_2, Ar]$ computed by SSH theory [20]–[24].
- vibration-vibration (VV) exchanges $N_2(X\ ^1\Sigma^+, v) + N_2(X\ ^1\Sigma^+, w) \rightleftharpoons N_2(X\ ^1\Sigma^+, v+1) + N_2(X\ ^1\Sigma^+, w-1)$ computed by SSH theory [20]–[24].

Backward rates are computed by applying the detailed balance principle. Rotational levels of each vibrational level are assumed to follow Boltzmann distributions at the rotational-translational temperature.
It should be noted that Esposito's rates have been computed for 68 vibrational levels. Our StS model comprises 45 vibrational levels for $N_2(X)$ because it is an extension of the collisional radiative model described in [17], [25]. The reactions rates of Esposito were then rescaled for these 45 levels, using the method explained in [26].

B. Results

3. *Temperature profiles*

The kinetic models required the temperature-time history $T(t)$ of the plasma along the tube centerline. This quantity was not measured directly because the measurement where performed at locations $x = 0, 10, 15\ [cm]$ along the tube centerline. To recover the temperature history, the velocity is required. Different velocity shapes $u(r)$ are assumed:

- constant $u(r) = cst$
- parabolic $u(r) = cst \cdot \left(1 - \frac{r}{R}\right)^2$
- from CFD simulations [27]

Constants are known by matching the mass flow rate. The more reliable velocity profile is the one based on CFD. Nevertheless, the others will be used as limiting cases, to provide error bars for our analysis. The computation of the velocity and temperature history profile is described in detail in [12], [13]. The same profiles have been chosen here because the mass flow rates of the recent experiments are almost identical as in the old experiments (less than 6% difference). Temperature history profiles are summarized in Table 3 for each assumed velocity profile.

Axial location $x\ [cm]$	Temperature $T\ [K]$	$t\ [\mu s]$ constant $U(r)$	$t\ [\mu s]$ CFD $U(r)$	$t\ [\mu s]$ Parabolic $U(r)$
0	6796 ± 100	0	0	0
10	4400 ± 500	247	169	112
15	3150 ± 400	405	276	184

Table 3 : Temperature history profiles

4. *Kinetics analysis*

The master equation at atmospheric pressure is solved by a "backward differential formulas" (BDF) method. The initial concentration profile is assumed to be at equilibrium for the inlet measured temperature, $T = 6796\ K$. The results are shown in Figure 2. On this figure, the experimental data points corresponding to the measured N densities are represented.

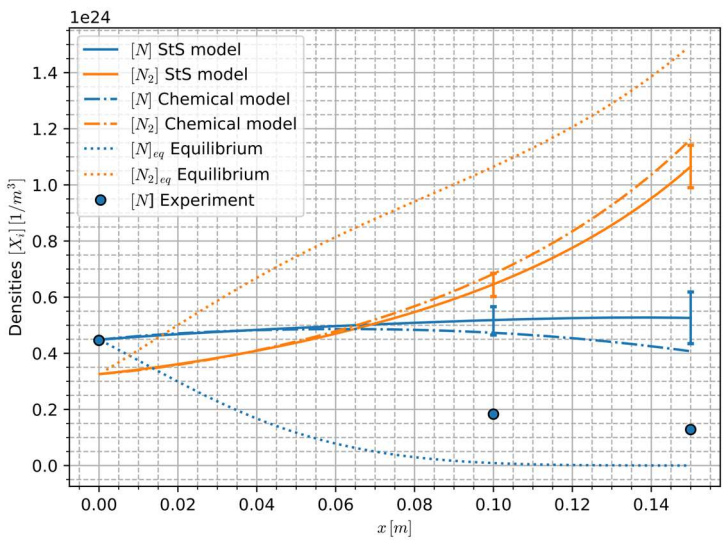

Figure 2 : Kinetic simulation of the chemical and StS model. The temperature history profile deduced by CFD simulation [27] **(see 4th column of Table 3) is used for the nominal calculation. The 2 other profiles (3rd and 5th column of Table 3) are used for the error bars.**

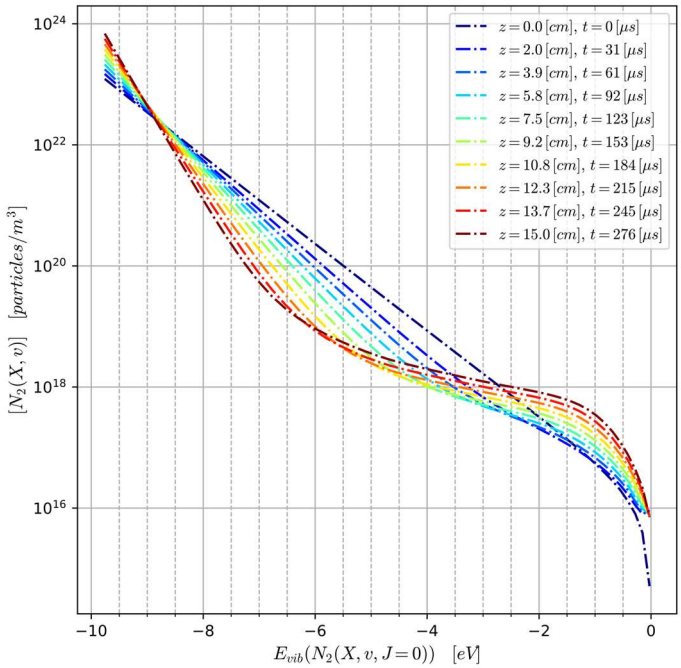

Figure 3 : Vibrational distribution of $N_2(X,v)$ levels as predicted by the StS model at different locations along the tube centerline

Both models are unable to match the measurements, as both underestimate the recombination of nitrogen atoms. The StS model prediction are worse than the chemical model. We should note that both models were found to converge to equilibrium when the calculations are run until very long times. For the StS model, the increase of N densities is explained by the increase of the total density (temperature drop at constant pressure). This difference can be explained by the slowdown of the cascade processes. In the StS model, N recombine preferentially in the high lying states, before cascading in the lower states. This is illustrated in Figure 3. High lying vibrational levels are then overpopulated, which slows down the recombination of over atoms. This phenomenon is not considered in the chemical model.

We ran another set of calculations with higher rates until we obtained agreement between the chemical model and the measurements, and then between the StS model and the measurements. In Figure 4, the rates of the chemical and StS models are multiplied by $f = 4$ so that the chemical model agrees with experimental data. In Figure 5, the rates have been multiplied by $f = 8.5$. Now the StS model predicts experimental data but the chemical model overpredicts the recombination of atomic nitrogen.

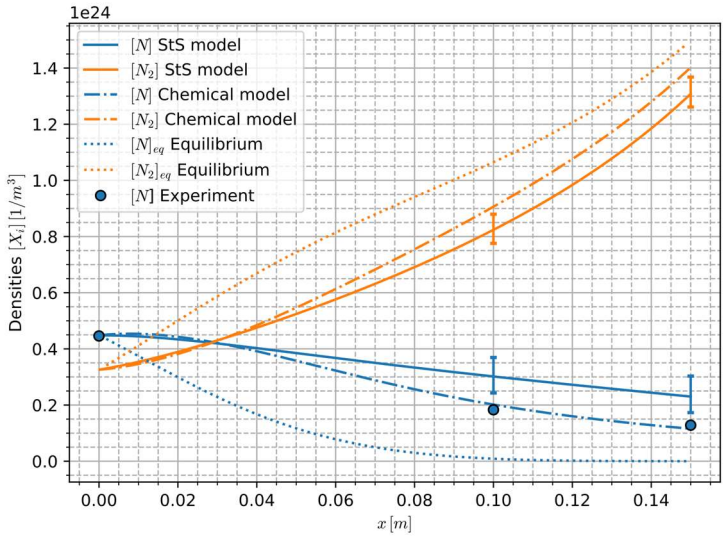

Figure 4 : Kinetic simulations of atomic and molecular nitrogen densities with the chemical and StS models whose rates are multiplied by $f = 4$. The temperature history profile deduced by CFD simulation [27] **(see 4th column of Table 3) is used for the nominal calculation. The 2 other profiles (3rd and 5th column of Table 3) are used for the error bars.**

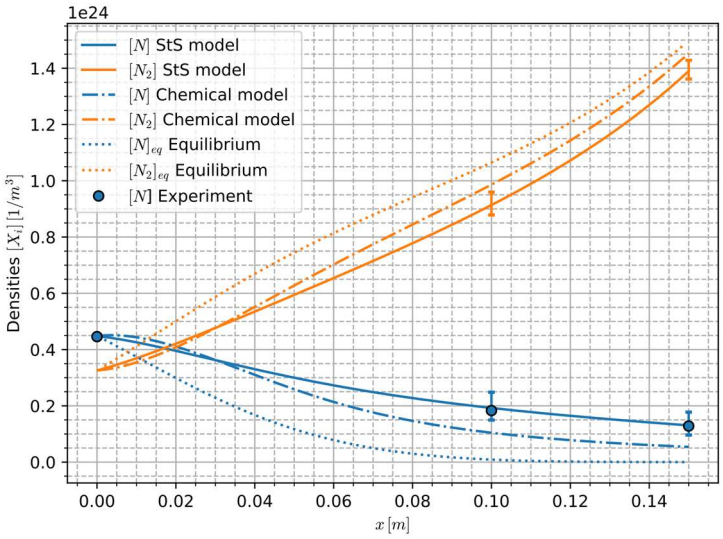

Figure 5 : Kinetic simulations of atomic and molecular nitrogen densities with the chemical and StS models whose rates are multiplied by $f = 8.5$. The temperature history profile deduced by CFD simulation [27] **(see 4th column of Table 3) is used for the nominal calculation. The 2 other profiles (3rd and 5th column of Table 3) are used for the error bars.**

IV. Conclusion

A comparison of recombination predictions obtained with a chemical and a state-to-state model was made against recent experimental data. It is shown that both models disagree with the measurements. To obtain agreement between the StS model and the experiments, the rate of $N + N + M$ recombination must be multiplied by a factor of about 8.5. Atomic nitrogen recombines faster with the chemical model than with the StS model because cascade from high vibrational levels is not considered in the chemical model. More work is required to understand the differences between the measurements and the simulations.

Acknowledgments

Augustin Tibère-Inglesse was supported by CIFRE grant number 42701092/20160218/JSE with ArianeGroup (technical monitor: Laurent Visconti).

References

[1] P. Jacobs and R. Gollan, "Implementation of a Compressible-Flow Simulation Code in the D Programming Language," *Appl. Mech. Mater.*, vol. 846, pp. 54–60, Jul. 2016.

[2] R. J. Gollan and P. A. Jacobs, "About the formulation, verification and validation of the hypersonic flow solver Eilmer," *Int. J. Numer. Methods Fluids*, vol. 73, no. 1, pp. 19–57, Sep. 2013.

[3] G. V. Candler, H. B. Johnson, I. Nompelis, V. M. Gidzak, P. K. Subbareddy, and M. Barnhardt, "Development of the US3D Code for Advanced Compressible and Reacting Flow Simulations," *53rd AIAA Aerosp. Sci. Meet.*, no. January, pp. 1–26, 2015.

[4] M. J. Wright, W. T., and N. Mangini, "Data parallel line relaxation (DPLR) code user manual; Acadia - Version 4.01.1," 2009.

[5] C. Park, J. T. Howe, R. L. Jaffe, G. V. Candler, and C. Park, "Review of Chemical-Kinetic Problems of Future NASA Missions I Earth Entries," *J. Thermophys. Heat Transf.*, vol. 7, no. 3, pp. 385–398, Jan. 1993.

[6] C. Park, J. T. Howe, R. L. Jaffe, and G. V. Candler, "Review of chemical-kinetic problems of future NASA missions. II - Mars entries," *J. Thermophys. Heat Transf.*, vol. 8, no. 1, pp. 9–23, Jan. 1994.

[7] C. Park, *Nonequilibrium Hypersonic Aerothermodynamics*. 1989.

[8] M. Panesi, R. L. Jaffe, D. W. Schwenke, and T. E. Magin, "Rovibrational internal energy transfer and dissociation of N[sub 2]([sup 1]Σ[sub g][sup +])−N([sup 4]S[sub u]) system in hypersonic flows," *J. Chem. Phys.*, vol. 138, no. 4, p. 044312, 2013.

[9] R. S. Chaudhry, J. D. Bender, T. E. Schwartzentruber, and G. V. Candler, "Quasiclassical Trajectory Analysis of Nitrogen for High-Temperature Chemical Kinetics," *J. Thermophys. Heat Transf.*, vol. 32, no. 4, pp. 833–845, Oct. 2018.

[10] F. Esposito, I. Armenise, and M. Capitelli, "N–N2 state to state vibrational-relaxation and dissociation rates based on quasiclassical calculations," *Chem. Phys.*, vol. 331, no. 1, pp. 1–8, Dec. 2006.

[11] C. Laux, R. Gessman, and C. Kruger, "Mechanisms of ionizational nonequilibrium in air and nitrogen plasmas," in *26th Plasmadynamics and Lasers Conference*, 1995, pp. 1–10.

[12] R. Gessman, C. Laux, C. Kruger, R. Gessman, C. Laux, and C. Kruger, "Experimental study of kinetic mechanisms of recombining atmospheric pressure air plasmas," in *28th Plasmadynamics and Lasers Conference*, 1997.

[13] R. J. Gessman, "An Experimental Investigation of the Effects of Chemical and Ionizational Equilibrium in Recombining Atmospheric Pressure Air Plasmas," Stanford University, 2000.

[14] A. C. Tibère-Inglesse, S. McGuire, and C. O. Laux, "Nonequilibrium radiation from a recombining nitrogen plasma," in *2018 AIAA Aerospace Sciences Meeting*, 2018.

[15] A. C. Tibère-Inglesse, S. McGuire, P. Mariotto, and C. O. Laux, "Validation cases for recombining nitrogen and air plasmas," *Plasma Sources Sci. Technol.*, Aug. 2018.

[16] A. C. Tibère-Inglesse, S. D. McGuire, P. Mariotto, and C. O. Laux, "Validation cases for recombining nitrogen and air plasmas," *Plasma Sources Sci. Technol.*, vol. 27, no. 11, p. 115010, Nov. 2018.

[17] C. O. Laux, L. Pierrot, and R. J. Gessman, "State-to-state modeling of a recombining nitrogen plasma experiment," *Chem. Phys.*, vol. 398, pp. 46–55, Apr. 2012.

[18] C. PARK, "Two-temperature interpretation of dissociation rate data for N2 and O2," in *26th Aerospace Sciences Meeting*, 1988, p. 26.

[19] B. J. Mcbride, S. Gordon, and M. Reno, "Coefficients for Calculating Thermodynamic and Transport Properties of Individual Species," *Nasa Tech. Memo.*, vol. 4513, no. NASA-TM-4513, p. 98, 1993.

[20] K. N. C. Bray, "Vibrational relaxation of anharmonic oscillator molecules: Relaxation under isothermal conditions," *J. Phys. B At. Mol. Physcis*, vol. 1, no. 4, pp. 705–717, 1968.

[21] D. Rapp and P. Englander-Golden, "Resonant and near-resonant vibrational-vibrational energy transfer between molecules in collisions," *J. Chem. Phys.*, vol. 40, no. 2, pp. 573–575, 1964.

[22] J. H. Kiefer, "Effect of VV Transfer on the Rate of Diatomic Dissociation," *J. Chem. Phys.*, vol. 57, no. 5, pp. 1938–1956, 1972.

[23] J. Keck and G. Carrier, "Diffusion Theory of Nonequilibrium Dissociation and Recombination," *J. Chem. Phys.*, vol. 43, no. 7, pp. 2284–2298, Oct. 1965.

[24] G. D. Billing and E. R. Fisher, "VV and VT rate coefficients in N2 by a quantum-classical model," *Chem. Phys.*, vol. 43, no. 3, pp. 395–401, Nov. 1979.

[25] L. Pierrot, L. Yu, R. Gessman, C. Laux, and C. Kruger, "Collisional-radiative modeling of nonequilibrium effects in nitrogen plasmas," in *30th Plasmadynamic and Lasers Conference*, 1999, no. c.

[26] G. Colonna, L. D. Pietanza, and M. Capitelli, "Recombination-Assisted Nitrogen Dissociation Rates Under Nonequilibrium Conditions," *J. Thermophys. Heat Transf.*, vol. 22, no. 3, pp. 399–406, 2008.

[27] G. V. Candler *et al.*, "Numerical simulation of a nonequilibrium nitrogen plasma experiment," *28th Plasmadynamics Lasers Conf.*, no. June 1998, Jun. 1997.